A Photon-Mapping Informed Chan-Vese Segmentation Algorithm to Enable Multispectral Sensing and Path-Planning in 3D Virtual Environments

Bruce Johnson Jason Isaacs
Naval Surface Warfare Center
Panama City Division
Panama City, USA
{bruce.a.johnson5,jason.c.isaacs1}@navy.mil

Hairong Qi
EECS Department
University of Tennessee
Knoxville, USA
hqi@utk.edu

Abstract

Understanding how to provide better surveillance in areas not viewable by visible light can arrive by modeling a virtual environment illuminated by photons in the non-visible spectrum and providing the mobile sensing platforms (MSPs) populating these environments with the tools to maximize their sensing capabilities. In order to enhance MSP sensing ability as well as enable MSP route path-planning, we propose a 3D segmentation algorithm based upon the Chan-Vese method to create a connected 3D mesh within the MSPs' photon-mapping-illuminated virtual environment. The resulting segmentation mesh's vertices contain more photons to be sensed by an MSP traversing the mesh than could have been sensed if the MSP had traveled elsewhere. The connectedness of the segmentation mesh gives the MSP uninterrupted travel through these highly-illuminated areas and allows for a variety of mission-planning scenarios. The initialization problem inherent to the Chan-Vese segmentation algorithm is overcome in a novel way by using output from an algorithm solving the art gallery problem to produce an initial segmentation curve comprised of vertices which are highly distinguished from their neighbors. The results of our segmentation algorithm enables an MSP to focus its attention on areas in the 3D environment that maximize the (non-)visible spectrum photons obtainable by their sensors or conversely explore areas have not been well-illuminated.

1. Introduction

In order to understand and enable greater surveillance capabilities in arbitrary environments, it is necessary to take into account the influence of sensing spectra extending beyond the visible range as well as provide paths for the mobile sensing platform (MSP) responsible for performing surveillance to follow. Having an MSP capable of sensing its surroundings while it traverses to fixed points of visitation (or *waypoints*) leads us to ask the following questions:

1) How do we decide what areas are illuminated and which are not in order to best determine what is able to be sensed by an MSP?
2) How do we inform the MSP's waypoint path planner such that it will traverse through those areas which are more (or less) illuminated?

In order to answer these questions we will use a particular form of global illumination for an MSP-populated virtual environment, namely *photon mapping* [1]. Photon mapping models the behavior of photons by treating them as particles representing minute fragments of the illuminating-energy emanating from a photon source. When a simulated photon representing some member of the electromagnetic spectrum touches a surface within a 3D virtual environment, it may be stored in a *photon map* (whose data structure is a *k*-d tree [2]). Photon storage depends upon that photon-touched surface's material properties. Photon mapping has proven itself to be rather versatile in its ability to provide realistic renderings of virtual environments and account for both participating media (such as water) [1] and electromagnetic spectra beyond the visible (such as infrared) [3]. The number of photons obtainable by an MSP at a point in space may be regarded as that point's *photon volume*. Conversely, if a point is not well-illuminated, it may be regarded as being *shadowed*.

When we say that we are performing segmentation, we mean that we are producing a connected 3D mesh within a 3D virtual environment such that those vertices comprising the mesh may serve as MSP waypoints affording a greater photon volume within the MSP's sensing range than waypoints who are not elements of the mesh. This segmentation mesh allows us to answer the above questions in the following manner:

1) The MSP's sensing capabilities can be determined by a measurement of the photon volume available within the MSP's sensing range at a particular vertex on the mesh and
2) MSP movement can be confined to those vertices on the segmentation mesh that provide the greatest (or least) photon volume.

The Chan-Vese segmentation algorithm [4] utilizes level-set functions [5] to implicitly represent a segmentation boundary. This algorithm has proven itself amenable to application to 2D images and 3D models [6] [7] [8]. In [6] they perform segmentation using multiple

discretization equations for solving the curvature term. In [7] they perform segmentation without the need to solve a PDE. In [8] they use multiple "smoothing terms" in order to control the evolution of the segmenting boundary. However, these segmented models have so far been confined to models depicting static scenes that reside in what is effectively a vacuum.

The contribution this paper makes is a 3D Chan-Vese segmentation method informed by the photon mapping algorithm to produce a connected mesh leading us to answering the questions given above while being able to take into account multiple spectra in less-than-perfect environments. This paper is organized in the following manner: in Section 2 we will discuss the nature of the photon mapping algorithm, in Section 3 we will discuss how photon mapping and the Chan-Vese segmentation algorithm may be combined, in Section 4 we will provide results of such a combination and a comparison with *k*-means, and, finally, in Section 5 we discuss our results and where this work may lead in the future.

2. Background on photon mapping

2.1. The first pass of the photon mapping algorithm

The first pass of the photon mapping algorithm consists of two steps: photon emission and photon scattering. In the first step, p photons are created and launched into the scene. The second step determines how the photons will behave when they interact with surfaces in the 3D scene.

As a photon gets scattered or *bounces* in the virtual environment, it will be possibly absorbed, transmitted or reflected. Determining whether a photon is absorbed, transmitted or reflected is accomplished by means of the *Russian roulette* Monte Carlo technique [9].

If we want to take into account the effect of photons that lie outside the bandwidth of visible light, the aforementioned Russian roulette technique allows us to do so. Let $\zeta \in [0, 1]$ be a uniformly distributed random variable and let d, s and t be the material's diffuse reflection, specular reflection and transmission coefficients, respectively. The photon is diffusely reflected if $\zeta \in [0, d]$, specularly reflected if $\zeta \in (d, s + d]$, transmitted if $\zeta \in (s + d, s + d + t]$, and absorbed if $\zeta \in (s + d + t, 1]$. Accommodating photons lying outside the bandwidth of visible light may be accomplished by adjusting the photon's probabilities of absorption, reflection and transmission when the photon interacts with a surface residing in the scene.

If we want to take into account the effects of participating media such as water, fog, rain, smoke and so forth, Jensen advocates the use of a *volume photon map* storing the photons' interaction with the participating media under consideration [1]. The photons who escape interaction with the participating media are stored in a *global photon map* per the rules explained above.

2.2. The second pass of the photon mapping algorithm

The second pass of the photon mapping algorithm uses the photons stored in a photon map for the purpose of rendering the scene. Traditional rendering is achieved by determining the total amount of energy radiated from a surface in the virtual environment intersected by a ray cast by a ray-tracer residing at some observation point. A query to a photon map yields those photons who contribute to the radiant energy - expressed as a color - found at that point of ray-intersection. A query conventionally takes the shape of a sphere (or *query-sphere*) of radius r centered at point x_o (or *query-point*).

The query-point and the ray's point of intersection on the radiating surface do not necessarily have to be equivalent. The query-sphere can be regarded as a means of gathering the aggregate number of perceptible photons found within that sphere and thus generating a photon volume. By using the photon mapping algorithm, we are now enabled with the ability to distinguish between areas with greater and lesser photon volume in a 3D environment while taking into consideration MSP-sensor attenuation due to environmental effects and multiple EM spectra.

In our application, we are concerned only with the first pass of the photon mapping algorithm as a means of understanding the effect of a photon on determining what may be sensed within a virtual environment. We are not concerned with using a photon map to help render the virtual environment.

3. Photon-Mapping Informed Chan-Vese segmentation

Our segmentation method relies upon the creation of a connected three-dimensional grid of points (or vertices) surrounding the virtual environment's 3D models such that these vertices sense more photons than would be sensed by elements not in the mesh. These points, or *MSP-observation points*, are waypoints in which an MSP may move to or remain stationed. Successful segmentation results in the creation of a mesh encompassing those MSP-observation points that possess greater photon volume within the MSP's sensing range than those who do not. Successful segmentation depends upon three things:

1) The construction of an MSP-observation grid,
2) The correct determination of the number of photons (or photon volume) capable of being sensed by the MSP occupying a grid point, and
3) Initialization of the Chan-Vese segmentation algorithm.

Once these three conditions are met, we may then segment the 3D virtual environment to obtain our desired results.

3.1. Construction of a mobile sensing platform observation grid

Let O be a set of points which comprise a surface and let it be a member of the compact subset $\Omega \subseteq \Re^d$. The set O is an *occluder* residing in *environment* Ω. The set $X = \Omega \backslash O$ is the set of points in which a (possibly) omnidirectional-sensing MSP may be stationed and $x_o \in X$ is some MSP-observer station. An MSP-observer grid $G \subseteq X$ is comprised of a sequence of points $g_0, g_1, \ldots g_n$ wherein element g_i is separated by its neighboring elements by some distance such that the distance does not exceed the boundaries of G. (This distance assumption ensures that at least one observer station is found within the confines of G. In our application, we assume an equal geodesic distance of one separating the grid points as well as full connectivity among the observer stations in G.)

3.2. Establishing visibility for a mobile sensing platform's observation point

Understanding which photons are responsible for contributing to an MSP's ability to perceive their surroundings and those that do not is a well-established problem in photon mapping and has been subject to consideration previously [1]. We use the name *photon culling* to describe the act of testing and removing those photons found within the query-sphere which do not contribute to photon volume.

One means of culling invisible photons is to perform a dot product test on the normal vector emanating from point of intersection of the photon and the query-point. If the dot product performed on the query-point and the normal emanating from the point upon which the photon resides is greater than 0, then the query-point and the point of intersection are connected to one another and thus visible to one another. This technique for photon culling is similar to what was proposed by Jensen in [1]. A summation of all photons visible at a grid point is that point's photon volume.

3.3. Establishing initial conditions for Chan-Vese segmentation

The establishment of the initial segmentation curve for the Chan-Vese segmentation method is of critical importance to the outcome of the segmentation. This topic has been considered previously in [5] and [10]. The essence of the initialization problem is expressed by the fact that if a local minimum is found at the beginning of the Chan-Vese segmentation method's execution, then the segmenting curve will not advance.

We propose a new means of establishing the Chan-Vese segmentation algorithm's initial condition. Since our goal is to construct a mesh that maximizes the photon volume sensed at the vertices comprising the mesh, our initial condition will be a curve comprised of connected waypoints that have a high sensed photon volume. To establish the waypoints comprising this initial segmentation curve, we will solve the art gallery problem (AGP) [11] using the SPOQ algorithm outlined in [12].

The AGP is posited by the mathematics community as the following question:

- What is the minimal number of observers necessary to ensure that the maximal number of points in environment Ω are observed?

In our case, we want to find the minimal number of observers necessary to ensure that the maximal number of *uniquely*-observable photon volume is obtained at a particular observation point. Having those MSP-observer stations that provide maximal uniquely-observed photon volume allows us to establish an initial segmentation curve that provides the highest probability of performing segmentation.

Given an environment Ω populated with a set of MSP-observer grid points, G, illuminated by p photons, the SPOQ algorithm produces j grid points $g_0 \ldots g_j \subseteq G$ which have the greatest uniquely-observed photon volume sensed by an MSP stationed at a grid point $g \in g_0 \ldots g_j$. The initial segmentation curve is created by connecting the grid points comprising $g_0 \ldots g_j$ by some means (such as Dijkstra's path-finding algorithm [13]) such that they form a closed curve. Since the Chan-Vese segmentation algorithm relies upon region competition of energy gradients as a means of evolving the segmentation curve [14], the establishment of an initialization curve comprised of MSP-observer grid points that are (highly) distinguished from neighboring grid point thus leads to a non-zero influence on the segmentation curve's evolution. Hence, by taking the effort to solve the art gallery problem, we can ensure a high likelihood of segmentation occurring.

3.4. Combining concepts

Given environment Ω containing MSP-observer grid points G, let the function $V{:}G \rightarrow \{0\} \cup \Re^+$ represent the photon volume obtained by some means at an element of G. Our goal is to find a minimum to the functional $F(\phi)$ provided by Mumford and Shah [15] for some function $\phi{:}G \rightarrow \Re$. In [5] Chan and Vese use Euler-Lagrange equations and the gradient descent method to produce the following partial differential equation for the level set function ϕ to minimize $F(\phi)$ at a particular time step t.

$$\phi_t = \tilde{\delta}_h(\phi)[\mu \cdot \kappa - (V - c_1)^2 + (V - c_2)^2] \qquad (1)$$

where ϕ_t is the level set representation of the evolving segmentation curve at some time step t, κ represents the segmentation curve's curvature and $\tilde{\delta}_h$ is the discrete delta function which ensures curve smoothness. In Chan and Vese's original paper, the value of $\tilde{\delta}_h$ was $\varepsilon/(\pi(\varepsilon^2 + \phi^2))$ where ε is a (small) positive constant. In our application, the value of $\tilde{\delta}_h$ is calculated by means of the algorithm provided by Smereka in [16]. The values of c_1 and c_2 are the region averages of V in the respective regions where $\phi \geq 0$ and $\phi < 0$.

We will now show how we solve the PDE in Eq. 1 numerically in three dimensions. Let $\phi^n_{i,j,k}$ denote the value of the evolving curve at MSP-observer grid point i,j,k at iterative step n. We use the following notation given by [5] for the spatial finite differences. We presume equal (i.e. geodesic) spacing $h = 1$ between grid points.

$$\Delta^x_+ \phi^n_{i,j,k} = \phi^n_{i+1,j,k} - \phi^n_{i,j,k} \quad (2)$$

$$\Delta^x_- \phi^n_{i,j,k} = \phi^n_{i,j,k} - \phi^n_{i-1,j,k} \quad (3)$$

$$\Delta^y_+ \phi^n_{i,j,k} = \phi^n_{i,j+1,k} - \phi^n_{i,j,k} \quad (4)$$

$$\Delta^y_- \phi^n_{i,j,k} = \phi^n_{i,j,k} - \phi^n_{i,j-1,k} \quad (5)$$

$$\Delta^z_+ \phi^n_{i,j,k} = \phi^n_{i,j,k+1} - \phi^n_{i,j,k} \quad (6)$$

$$\Delta^z_- \phi^n_{i,j,k} = \phi^n_{i,j,k} - \phi^n_{i,j,k-1} \quad (7)$$

In order to simplify the notation used in our equations for expressing the solution to the discretized version of Eq. (1), we use the following finite central differences which are inspired by [8]:

$$\Delta^x \phi^n_{i+1/2,j,k} = \phi^n_{i+1,j+1,k} + \phi^n_{i,j+1,k} - \phi^n_{i,j-1,k} - \phi^n_{i+1,j-1,k} \quad (8)$$

$$\Delta^y \phi^n_{i+1/2,j,k} = \phi^n_{i+1,j+1,k} + \phi^n_{i+1,j,k} - \phi^n_{i-1,j+1,k} - \phi^n_{i-1,j,k} \quad (9)$$

$$\Delta^z \phi^n_{i+1/2,j,k} = \phi^n_{i+1,j,k+1} + \phi^n_{i+1,j,k} - \phi^n_{i-1,j,k} - \phi^n_{i-1,j,k+1} \quad (10)$$

The remaining central difference formulations follow a pattern similar to that shown above.

Let m_x, m_y and m_z be the number of points of grid G in the x, y and z directions, respectively. The von Neumann boundary conditions apply namely:

$$\phi^n_{0,j,k} = \phi^n_{1,j,k}, \phi^n_{m_x,j,k} = \phi^n_{m_x-1,j,k} \quad (11)$$

$$\phi^n_{i,0,k} = \phi^n_{i,1,k}, \phi^n_{i,m_y,k} = \phi^n_{i,m_y-1,k} \quad (12)$$

$$\phi^n_{i,j,0} = \phi^n_{i,j,1}, \phi^n_{i,j,m_z} = \phi^n_{i,j,m_z-1} \quad (13)$$

We use the following variable in order to streamline our notation of the iterative, numerical solution to ϕ^{n+1}:

$$C_1 = \left(\left(\Delta^x_+ \phi^n_{i,j,k}\right)^2 + \frac{\left(\Delta^x \phi^n_{i+1/2,j,k}\right)^2}{4} + \frac{\left(\Delta^x \phi^n_{i,j,k+1/2}\right)^2}{4} \right)^{-\frac{1}{2}} \quad (14)$$

The variables C_2, C_3, C_4, C_5 and C_6 follow a similar pattern to that shown above in the sense that the first element in the summation is $\left(\Delta^x_- \phi^n_{i,j,k}\right)^2$, $\left(\Delta^y_+ \phi^n_{i,j,k}\right)^2$, $\left(\Delta^y_- \phi^n_{i,j,k}\right)^2$, $\left(\Delta^z_+ \phi^n_{i,j,k}\right)^2$, and $\left(\Delta^z_- \phi^n_{i,j,k}\right)^2$ respectively. The second and third elements in the summation conform to a similar pattern as that shown in C_1.

The method advocated in [17] provides us with the following iterative solution to ϕ^{n+1}:

$$\phi^{n+1}_{i,j,k} = F_1 \phi^{n+1}_{i+1,j,k} + F_2 \phi^{n+1}_{i-1,j,k} + F_3 \phi^{n+1}_{i,j+1,k} + F_4 \phi^{n+1}_{i,j-1,k} + F_5 \phi^{n+1}_{i,j,k+1} + F_6 \phi^{n+1}_{i,j,k-1} + F w_{i,j,k} \quad (15)$$

where

$$F_l = \frac{\Delta t \tilde{\delta}_h\left(\phi^n_{i,j,k}\right) \mu (p \cdot L(\phi^n)^{p-1}) C_l}{h + \Delta t \tilde{\delta}_h\left(\phi^n_{i,j,k}\right) \mu (p \cdot L(\phi^n)^{p-1}) \left(\sum_{g=1}^{6} C_g\right)} \quad (16)$$

for $l = 1, 2, 3, 4, 5, 6,$ and

$$F = \frac{h}{h + \Delta t \tilde{\delta}_h\left(\phi^n_{i,j,k}\right) \mu (p \cdot L(\phi^n)^{p-1}) \left(\sum_{g=1}^{6} C_g\right)} \quad (17)$$

and the error factor $w_{i,j,k}$ is

$$w_{i,j,k} = \phi^n_{i,j,k} - \Delta t \tilde{\delta}_h\left(\phi^n_{i,j,k}\right)\left(\nu\lambda_1\left(G^v_{i,j,k} - c_1(\phi^n)\right)^2 - \lambda_2\left(G^v_{i,j,k} - c_2(\phi^n)\right)^2\right) \quad (18)$$

The variable $L(\phi^n)$ is the surface area of the segmentation mesh and the formula for its calculation is:

$$L(\phi^n) = \int_G \tilde{\delta}_h(\phi^n) |\nabla \phi^n| dx dy dz. \quad (19)$$

The delta function $\tilde{\delta}_h$ serves to smooth the segmentation mesh as it evolves. For details regarding its calculation, please refer to [16].

The steps for our algorithm are given below:

1. Construct a 3D model of the virtual environment
2. Construct the MSP-observer grid G
3. Apply the photon mapping algorithm to the virtual environment using photons of the EM spectrum desired
4. Obtain the photon volume sensed at every grid point $g_i \in G$
5. Utilize SPOQ in the manner described above in order to establish the initial condition $\phi^0_{i,j,k}$ to the Chan-Vese segmentation algorithm.
6. Apply the iterative solution to $\phi^{n+1}_{i,j,k}$ given by Eq. (15) using the initial conditions established in step 5.

4. Results and discussion

To demonstrate the efficacy of our algorithm, we applied it to the following scenarios:

1. Using 14000 photons cast and 1020 observer grid points
2. Using 7000 photons cast and 1020 grid points,
3. Using 14000 photons cast and using 6897 grid points, and
4. Using 7000 photons cast and 6897 grid points.

The first scenario may be regarded as a "baseline", the second scenario represents a low photon count (i.e. dim) environment and the last two scenarios demonstrate the scalability of the algorithm to more complicated grids.

Figure 1 shows the output of our segmentation algorithm operating in the circumstances described by scenario 1 and applied to a 3D virtual environment representing a stylized urban scene. (Note that the scene's simplicity was chosen to make the resulting Chan-Vese segmentation mesh more visible.)

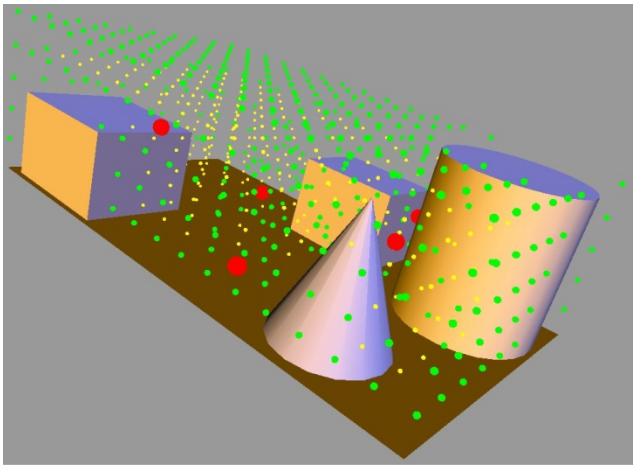

Figure 1: The result of our Chan-Vese algorithm. The green vertices are in the segmentation mesh, yellow vertices are not in the mesh and red vertices solve the AGP.

The following tables show the performance of our algorithm as applied to the scenarios described above. In each case, the Chan-Vese algorithm was compared to a *k*-means classifier arriving from the ITK toolkit [18] that clusters around "light" and "dark" grid points. The elements that *k*-means operates on consists of an array of size $|G|$ wherein the ith element corresponds to element $g_i \in G$ and that element's value is g_i's photon volume. The initial mean value of the cluster of "light" grid points arrives from the photon volume of those points used as the initial condition to the Chan-Vese algorithm. The resulting segmentation mesh provides a set of bright grid elements where the most photons may be sensed. This mesh was compared with our Chan-Vese algorithm's mesh.

Table 1 shows the respective algorithms' ability to perceive photons and timing. Table 2 shows the respective segmentation meshes' "connectivity" which is the cardinality of the largest set of connected vertices provided by the `connected_components()` algorithm implemented in the boost graph library [19]. The connectivity number represents the number of candidate waypoints that may be traversed by an MSP in the respective segmentation meshes. Hence, a higher connectivity count is better as it indicates that a greater number of paths may be chosen by an MSP to realize multiple mission scenarios.

The first table indicates that while *k*-means is faster and produces a greater sensed photon volume per mesh vertex, the total number of photons available to be observed is similar to that provided by the Chan-Vese segmentation algorithm. (Note that an observation point within a mesh may have overlapping surveillance with a neighboring point.) The strength of the Chan-Vese algorithm is demonstrated in Table 2 as it produces a larger set of candidate way points that may be traversed by an MSP thus allowing for a greater number of possible mission applications while maintaining a high degree of surveillance capability as the MSP traverses these waypoints.

Segmentation Method	Photon Volume per Vertex	Percentage of all available photons viewed	Timing (sec)	Scenario
Chan-Vese	1221.5	92.3	0.06	1
k-means	3770.3	91.4	0.001	
Chan-Vese	1170.7	91	0.05	2
k -means	3690.4	89	0.001	
Chan-Vese	1661.1	96	0.47	3
k -means	3655.1	94.5	0.004	
Chan-Vese	1658.1	95.3	0.45	4
k -means	3652.3	94.3	0.003	

Table 1: Comparison of Chan-Vese and *k* -means segmentation in terms of photon volume per vertex, percentage of photons perceived and timing.

Segmentation Method	Connectivity	Percentage Improvement of Chan-Vese over *k* -Means	Scenario
Chan-Vese	435	65	1
k-means	151		
Chan-Vese	433	65	2
k-means	151		
Chan-Vese	3090	40	3
k-means	1846		
Chan-Vese	3084	40	4
k-means	1844		

Table 2: Comparison of Chan-Vese and *k*-means segmentation in terms of connectivity.

5. Conclusions and future work

We have presented a segmentation algorithm for determining where MSPs may traverse in a 3D virtual environment such that the maximal amount of information (represented as a multi-spectral photon volume) may be obtained. The significance of this effort is that it enables the realization applications answering the questions asked in the Introduction in multi-spectral 3D environments which may then be affected by information-attenuating events such as simulated fog, rain, and so forth.

The *k*-means algorithm confines the MSP movement to a small subset of the MSP-observer grid. However, the *k*-means algorithm can also serve as a method of performing pre-segmentation of an MSP-observer grid so as to identify those portions of the MSP-observer grid that possess greater and lesser amounts of multi-spectral photon volume. This pre-segmented mesh can then allow for multi-MSP path planning as the Chan-Vese segmentation algorithm can then be applied to the pre-segmented MSP-observer sub-grids. This resulting set of candidate waypoints can then be assigned that sub-grid's MSP. The concept of pre-segmentation by *k*-means in order to inform Chan-Vese arrives from [20].

A future application we would like to pursue entails *phonon mapping* [21]. The photon mapping algorithm's photon map construction need not be confined strictly to the EM spectrum. Extending the concept of the photon to be any discrete packet of information-bearing energy propagating through a medium, the behavior of sound traversing through air can also be modeled. This packet of sound energy is known as a *phonon* rather than a photon. While the phonon's operational characteristics in air have been considered previously, the transmission of a phonon through water has not been done.

Acknowledgements

We would like to thank Dr. Quyen Hyuhn of NSWC PCD for his generous support from NSWC PCD's In-House Laboratory Independent Research (ILIR) program.

References

[1] H.W. Jensen, *Realistic Image Synthesis Using Photon Mapping*. New York, NY: A. K. Peters, 2001.

[2] T. H. Cormen, C. E. Leiserson, R. L. Rivest, and C. Stein, *Introduction to Algorithms 3rd Edition*. Cambridge, MA.: MIT Press, 2009.

[3] A. Goodenough, R. Raqueno, M. Bellandi, S. Brown, and J. A. Schott, Flexible hyperspectral simulation tool for complex littoral environments, *Proceedings of SPIE*, Vol. 6204, 2006.

[4] T. Chan and L. Vese, Active contours without edges, *IEEE Transactions on Image Processing* 10(2), pp. 266-277, 2001.

[5] J. A. Sethian, "Tracking interfaces with level sets", *American Scientist*, pp 254-263, May-June, 1997.

[6] O. Rousseau and Y. Bourgault, An iterative active contour algorithm applied to heart segmentation. *SIAM Conference on Imaging Science*. San Diego, CA, 7-9 July, 2008.

[7] D. Jianyuan and H. Chongyang, 3D fast level set image segmentation based on Chan Vese model, 3rd *International Conference on Bioinformatics and Biomedical Engineering*. Beijing, China, June 11-13 2009.

[8] J. Zhang, K. Chen and B. Yu, A 3D multi-grid algorithm for the Chan-Vese model of variational image segmentation. *International Journal of Computer Mathematics* 89(2), pp 160-189, 2012.

[9] J. Avro and D. B. Kirk, Particle transport and image synthesis in computer graphics (*Siggraph* '90) 24(4): 63 – 66, 1990.

[10] B. Johnson and Y. Pan, A sensitivity analysis of initial conditions for the Mumford-Shah based level set method of image segmentation. *Proceedings of the ACM Southeast Conference* (*ACMSE* 2007), Winston-Salem, NC. March 23-24, 2007.

[11] R. Goroshin, Q. Huynh, and H. M. Zhou, Approximate solutions to several visibility optimization problems. *Communications in Mathematical Sciences*, 9(2), 535-550, 2011.

[12] B. Johnson, H. Qi and J. Isaacs, Optimizing coverage of three-dimensional wireless sensor networks by means of photon mapping. *Proceedings of the Winter Simulation Conference* (*WSC* 2013), Washington, DC. Dec 8-11, 2013.

[13] E. W. Djikstra, A note on two problems in connexion with graphs, *Numerische Mathematik* 1(1), pp 269-271, 1959.

[14] Y. Pan, J. D. Birdwell, S. M. Djouadi, Efficient bottum up image segmentation using region competition and the Mumford Shah model for color and textured images. *Eigth IEEE Internation Smposium on Multimedia* (*ISM* '06), San Diego, CA Dec 11-13, 2006.

[15] D. Mumford and J. Shah, Optimal approximation by piecewise smooth functions and associated variational problems, *Comm. Pure and Applied Math*. 42, pp. 577-685, 1989.

[16] P. Smereka, The numerical approximation of a delta function with application to level set methods. *J. of Comp Physics*, 211(1), pp. 77-90, 2006.

[17] G. Aubert and L. Vese, A variational method in image recovery, *SIAM J. Num. Analysis*., 34(5), pp. 1948-1979, 1997.

[18] http://www.itk.org

[19] http://www.boost.org

[20] S. Gao, J. Yang and Y. Yan, A local modified Chan-Vese model for segmenting inhomogeneous multiphase images. International *Journal of Imaging Systems and Technology* 2(2), pp 103-113, June 2012.

[21] B. De Greve, T. Willems, T. De Muer, and D. Botteldooren, The effect of diffuse reflections on noise maps using phonon mapping. *The* 13*th International Congress on Sound and Vibration* (*ICSV* 13), Vienna, Austria, Jul 2-6, 2006.